Fluid Flow in Metals Processing: Achievements of CFD and Opportunities

J. W. Evans

Department of Materials Science and Mineral Engineering
University of California, Berkeley CA, USA

ABSTRACT

The paper examines the application of computational fluid dynamics in metals processing operations. It is shown that, even within a subset of the metallurgical literature, papers on CFD in process metallurgy are legion. The common approaches of these papers (e.g., widespread use of the k-ε model for turbulence) are shown using the examples of gas-stirred melts and flow in continuous casters (including tundishes). The paper ends with a discussion of two areas (free surface problems and flow at the level of the microstructure during solidification) where there appear to be major opportunities for the application of CFD.

1. INTRODUCTION AND OBJECTIVE

Application of CFD in metals processing is now over twenty years old (e.g., Szekely et al., 1976, Tarapore and Evans, 1976) and has become widespread. A very casual survey by the author showed that in the past three years, two major journals in the field (ISIJ International and Metallurgical and Materials Transactions B) have published nearly fifty papers involving CFD. Flow in continuous casters is treated in the largest group (twelve) of papers, with an additional five papers on flow in tundishes (one related to aluminum casting). The next largest groups are gas stirred flows and MHD flows (eight each). Application of CFD in fundamental studies of solidification (four papers) can be found along with a variety of other topics such as high speed or strip casting or the processing of composites. The vast majority of the computed flows depicted in these papers are credible and many show very good match to experimental data. This then is an achievement that will be examined in more detail below using a few examples from the literature. Two areas where CFD may provide an opportunity for advancement of technology are the behavior of interfaces (free surfaces and liquid/liquid interfaces) and solidification microstructure/ chemistry; the paper closes with some thoughts on these opportunities.

2. ACHIEVEMENTS OF CFD IN PROCESS METALLURGY

As examples of the progress made in computing flows in metallurgical unit operations, gas stirring of melts and the flow in continuous casters will be considered.

2.1 Gas-stirred melts

Mazumdar and Guthrie (1995) have recently reviewed the physical and mathematical modeling of gas stirred systems of which the argon stirred ladle in the steel industry is probably the best known example. These ladles are stirred by gas injection (usually through a porous plug at the center of the bottom of the ladle) and the buoyancy of the rising plume of gas brings about a recirculating flow of metal. Computation of the flow is made difficult by the fact that it is turbulent and two phase (three phase if there is a slag cover on the metal). It is driven by the bubble plume which has poorly understood characteristics that are dependent on the injection method, bubble coalescence or breakup, as well as on the melt flow. The flows can be three dimensional (e.g. for off-axis injection) and transient (in more than the sense of turbulence). They are beneath a free surface which is made non flat by the upwelling melt.

Because of the difficulty of making velocity measurements on large hot melts, much of the experimental data with which computations are compared have been obtained on water models. An early success in computing these flows was that of Sahai and Guthrie (1982) shown in Figure 1. Here the quasi single phase approach was used whereby the plume region was treated in the same way as the surrounding gas free annulus, except that it was assigned a reduced density dependent on the gas velocity and plume geometry. The plume geometry was determined in the water model and input into the calculations of Sahai and Guthrie. More detailed and more predictive treatments of the plume region have been carried out in recent years. Some of these have avoided the simplistic treatment entailed in single phase models. One approach (referred to by Mazumdar and Guthrie as the "two-phase

Eulerian approach") is to write separate continuity and momentum equations for each phase. Each momentum equation then contains a body force representing the drag due to the relative velocity between phases. A drag coefficient is invoked to obtain this force and the characteristics of the bubbles (e.g., their Reynolds number) thereby incorporated in the model.

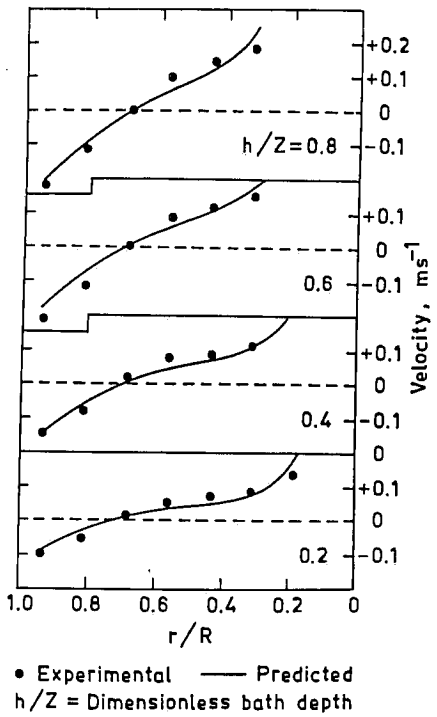

Fig. 1: Comparison of experimentally measured and theoretically predicted vertical velocity component at different depths in a water model ladle. The work of Sahai and Guthrie (1982).

A third approach ("two-phase Lagrangian") is to solve the continuity and momentum equations (with terms modified as in the 2 phase Eulerian method, e.g. to allow for a variable gas fraction) and then to calculate the local gas fraction by solving an (ordinary differential) equation for the of trajectory of a bubble. As in the second approach, this third approach permits the incorporation of bubble characteristics through a drag coefficient. It has been usual to treat turbulence in the liquid phase by a traditional model, such as the k-ε model, in some cases with extra source terms in the turbulence equations to account for the generation of turbulence by the bubbles. Mazumdar and Guthrie (1994) have compared the results of the three approaches with experimental data and Figs. 2 and 3 are taken from that comparison. It is seen that all three approaches agree quite well with the experimental data both with respect to the time averaged velocity and the turbulence. It should be recognized however that this need not always be the case as seen in Table I from Mazumdar et al. (1993). Furthermore, the quasi single phase approach requires much more by way of empirical input (plume geometry) than the other two approaches. Its application to the opaque high temperature melts encountered in process metallurgy therefore appears a little risky to this author.

Zhu and coworkers (1995, 1996) have carried out three dimensional calculations using the quasi single phase approach. The ladles under consideration were ones where gas was injected at multiple or off-center points at the bottom of the ladle. The bubble plume was described based on the work of Castillejos and Brimacombe (1989) and turbulence was treated using the standard k-ε model. Figure 4 is a comparison of the vertical velocities computed by these authors and the measurements of Mietz and Oeters (10). These results are for a vertical plane containing the gas injection point and the fit of the computations to the data is a good example of the achievement of CFD in process metallurgy.

Jonsson and Jönsson (1996) have employed the Eulerian two phase model to treat flow in gas stirred ladles. Furthermore they modeled the flow in the slag phase above the steel melt. The equations were solved using the well known software Phoenics. Figure 5 is one result of these investigators showing the velocities on both sides of the slag metal interface.

An example of a recent application of the two phase Lagrangian approach in gas stirred systems is the work of Sheng and Irons (1995). In this exemplary investigation, these workers carried out extensive measurements of bubble and liquid velocity, void fraction and turbulence levels in a water model using laser-Doppler velocimetry (LDV) and an electroresistivity probe. Their calculations treated the turbulence by means of a k-ε model modified to allow for bubble generated turbulence. Allowance was also made for breakup of bubbles and predictions with breakup of bubbles excluded were found inaccurate. Liquid velocities along the plume centerline, as measured and calculated by these authors, appear in Figure 6. The ability to even make these measurements (where gas fraction is highest) is remarkable; the agreement of the calculated results is a substantial achievement.

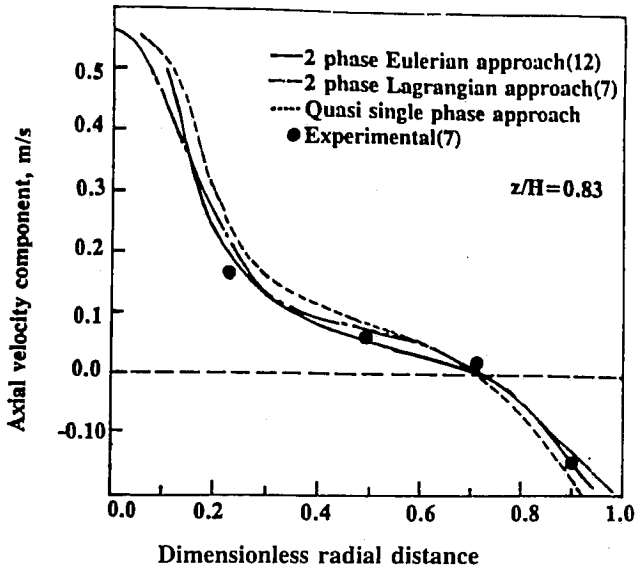

Fig. 2: Numerically predicted axial velocity and corresponding measurements illustrating a comparison between the two-phase and quasi single-phase calculation procedures as reported by Mazumdar and Guthrie (1994).

Gas flow rate $x10^5$, m^3/s	Turbulence kinetic energy $x10^4$, m^2/s^2		Turbulence intensity		Turbulence energy dissipation rate, $x10^4$, m^2/s^2	
	Experimental	Predicted	Experimental	Predicted	Experimental	Predicted
1.66	0.824	7.3	0.218	0.51	6.23	3.95
3.33	2.0	8.8	0.254	0.52	12.5	5.9
5.0	2.39	14.6	0.236	0.52	18.7	11.7

Table I
Numerically predicted (via standard coefficient k-ε turbulence model) bulk average values of v arious turbulence quantities in a gas stirred bath (L=0.21m, D=0.15m) as functions of gas flow rates and their comparison with corresponding experimental measurements. Mazumdar et al. (1993)

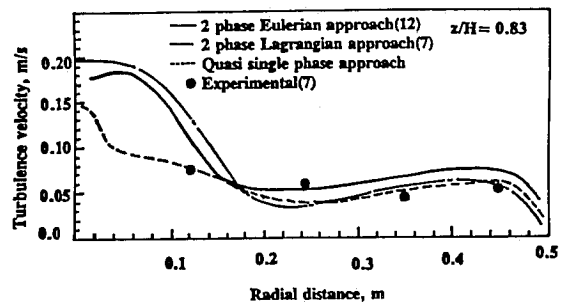

Fig. 3: Numerically predicted isotropic turbulence velocity and corresponding measurements illustrating a comparison between the two-phase and quasi single-phase calculation procedures. Work of Mazumdar and Guthrie (1994).

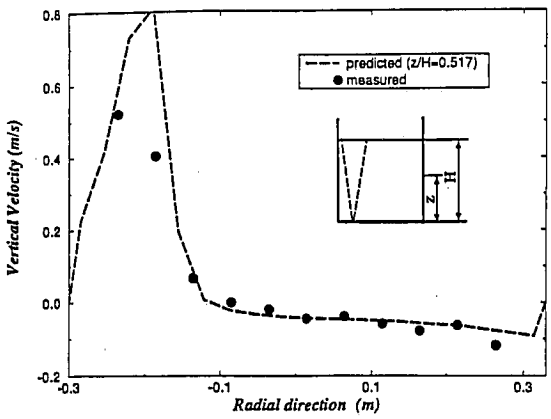

Fig. 4: Predicted axial velocities of Zhu and coworkers (1996) compared to measurements of Mietz and Oeters (1989).

It should now be clear that the characteristics of the bubbles and plume are significant in determining the flow in gas stirred melts. Fortunately much is now known concerning bubble size, velocity and dispersion in gas injection into liquids. Electroresistivity probes (where the passage of a bubble past the conducting tip of a probe breaks an electrical circuit) have found widespread use in bubble studies since the pioneering work of Castillejos and Brimacombe (1987). Most such investigations have been confined to water, although some measurements have been done in molten metals (e.g., Castillejos and Brimacombe, 1989, Iguchi et al., 1995). Water has been a convenient model fluid for measurements using LDV such as that of Sheng and Irons cited above or the several investigations of Iguchi et al. (1995-1997).

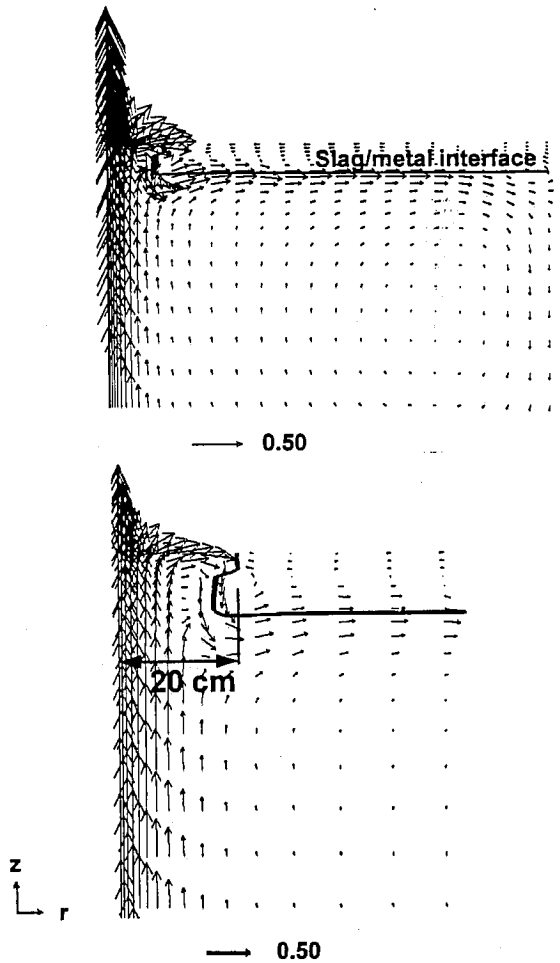

Fig. 5: Velocity vector plots for the region close to the plume for a 160 l/min gas flow. The heat size and ladle radius are 100 t and 1.5 m, respectively. Jonsson and Jönsson (1996).

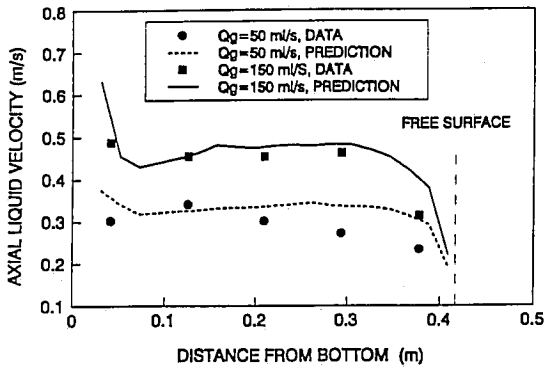

Fig. 6 : Comparison of predicted and measured axial liquid velocity along the plume centerline from the work of Sheng and Irons (1995).

Of course, the flow within gas stirred melts is not only significant in its own right ,but also as it affects mass and heat transport. Notable work in this area has been done by Singh and Mazumdar (1997) who correlated their experimental measurements of the rate of dissolution of benzoic acid into gas stirred water with both measured (by LDV) and computed velocity and turbulence levels. Their correlation appears in Fig 7.

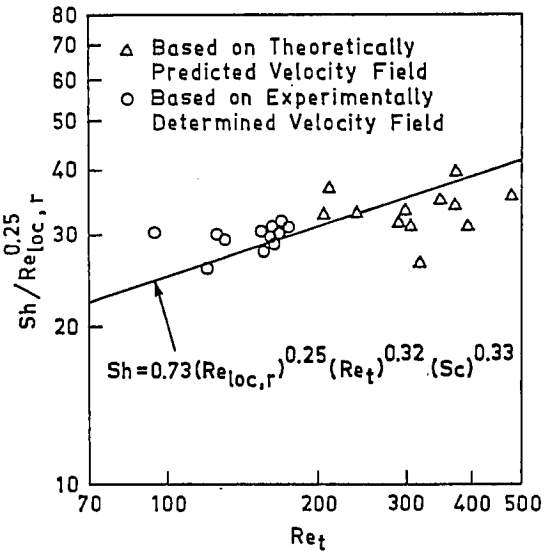

Fig. 7: Sherwood numbers for mass transfer as a function of turbulence Reynolds number for gas-stirred melts, from Singh and Mazumdar (1997).

2.2 Continuous casting

Continuous casting is now the established technology for casting of steel although competition has emerged in the form of a variant (thin slab casting) and various high speed casting technologies such as twin roll casting may offer further competition. Steel flows into the caster via a tundish and a submerged entry nozzle (SEN) leading into a water cooled copper mold from the bottom of which the steel, now with a solidified steel shell is withdrawn for further solidification/ cooling. The "direct chill" (DC) casting of aluminum is somewhat similar, the differences (e.g. oscillating mold in the steel case) mostly having to do with mechanics, rather than fluid mechanics.

Fluid flow within the continuous caster has many significant effects such as the flotation or entrapment of inclusions, heat transport to the solidified shell (with consequences ranging from breakout to deformation under thermal stresses), behavior of the "flux" powder used to lubricate the steel/mold interface, and microstructure/segregation of the solidified metal. For this reason continuous casting was one of the first unit operations studied by CFD and physical modeling (e.g., the work of Szekely and Yadoya (1972, 1973)). Since that time there have been many fruitful investigations and only a few recent ones are mentioned here.

The fluid dynamicist doing calculations on continuous casters (as opposed to tundishes) is blessed with a relatively simple geometry because in the region of interest the solid shell is sufficiently thin that it can be ignored giving a volume approximating a cuboid. [The same would not be true for DC casting where the low casting speeds and significant axial heat flux result in a relatively shallow pool of molten metal; see for example Prasso and Evans (1996)]. Furthermore, although the flow is turbulent, it is highly turbulent, even well below the mold region (Thomas et al., 1994), and the high inlet velocity at the nozzle (of the order of a meter per second), coupled with the high density, makes inertial terms dominant and should lead to successful velocity predictions even with the simplest turbulence model. Complications include the flux (always used), argon injection into the SEN (frequently used to minimize nozzle blockage arising from oxidation products produced by air entering the SEN) and the imposition of electromagnetic braking or stirring (frequently in use in Japan).

An example of 3D calculations carried out for the case of no argon or electromagnetic forces is the work of Ho et al. (1994) with one result depicted in Figure 8. One half of the caster is shown with the SEN (idealized here as square in cross section but in reality circular) to the left. The SEN has two exit ports (one seen in this half) directing the inflow jet horizontally to the short side of the caster, as is usual practice. Two recirculation loops, one above the ports and one below are computed (using the k-ε model), in line with the results of earlier workers. These workers went on to studied the effect of various port tilt angles (inclinations of the port axis to the horizontal) and submergence depths, particularly with respect to the escape of less dense inclusions carried into the pool by the steel.

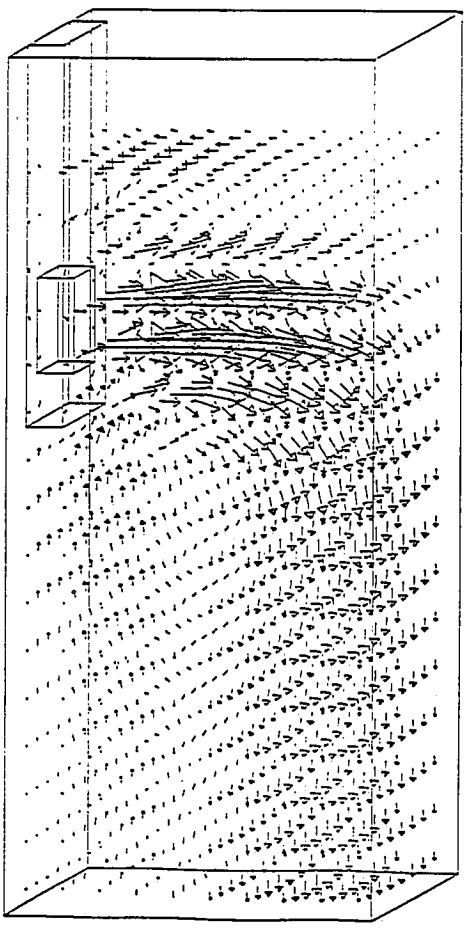

Fig. 8: Calculated flow pattern in right half of mold from the work of Ho et al. (1994).

Najjar and coworkers (1995) have also performed CFD calculations (k-ε) for various tilt angles, concentrating their efforts on flow just outside the port and in the SEN itself. Figure 9 is representative of their results and shows the propensity for the flow to exit the bottom of the port. Rather an unusual nozzle flow, one where swirl is induced (e.g. by electromagnetic forces) in a divergent SEN has been examined by Yokoya et al. (1994). Experimental measurements on a water model were carried out by LDV and in a subsequent paper (Yokoya et al., 1994b) the k-ε model was used in calculations of the velocity, which is predominantly in the radial direction at high swirl numbers. A sample comparison of calculated and measured velocities appears in Figure 10 and agreement is seen to be good. A solid surface (representing, say, a solidification front onto which jet impingement is to be minimized) is at 22mm below the nozzle (which is at the top). It is seen that as the swirl is increased the radial flow shifts upward away from this surface in both the calculations and measurements.

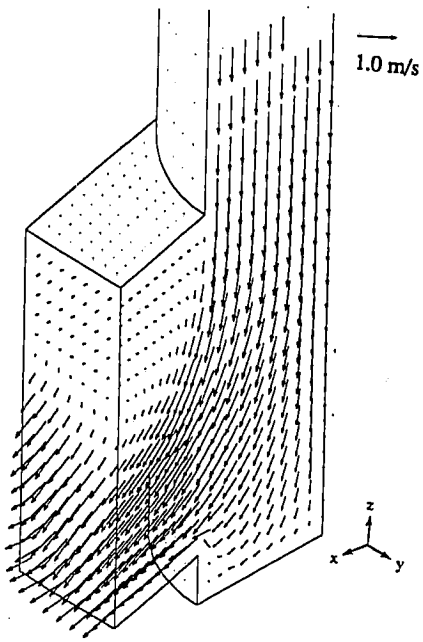

Fig. 9: Flow at the exit of the SEN, from Najjar et al. (1995).

The effect of argon injection on the flow was calculated by Thomas and colleagues (1994) using a quasi single phase model but with an interesting treatment of the bubbles that minimized empirical input. This treatment was similar to that of Ziegler and Evans (1986) in a different application (bubble driven flow in an electrowinning cell). The bubbles were regarded as a solute which was convected by the time average motion (with allowance for the bubble rise, at the terminal velocity, with respect to the liquid) and dispersed by turbulence (with a turbulent Schmidt number of unity). The calculated flow was three dimensional and agreement between calculated and measured (by hot film velocimetry) liquid speeds in a water model can be seen in Figure 11. Both results, which are for the case of no argon, show the strong jet emerging from the port (angled 25 degrees downwards from horizontal) and dissipating as it moves outwards (to the right in the figure). Computed results show that argon deflects the jet upwards due to buoyancy effects although the experimental measurements were not carried out at a high enough gas fraction to make this evident. These workers went on to examine the effect of argon flow on heat and mass transport, including the effect when the grade (composition) of the steel is changed, the intention being to minimize the length of steel cast with intermediate composition. Flow in the flux on the top of the molten steel has been the subject of recent (laminar) calculations by McDavid and Thomas (1996). A difficulty faced by these investigators is that the viscosity of the fluxes is temperature dependent so that the flow equations had to be solved simultaneously with heat transport equations. The boundary conditions on the lower surface of the flux arose from 3D computations of the steel flow similar to those described earlier in this section.

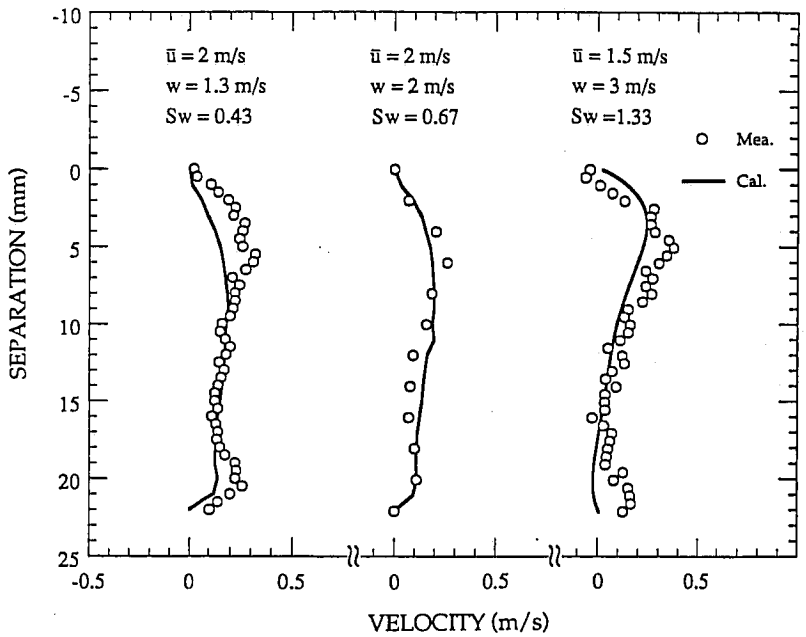

Fig. 10: Comparison between the calculated (solid line) and the experimentally measured (symbols) profiles of the radial velocity at the nozzle outlet, with the swirl strengths denoted by the inlet tangential velocity, w for the case: u, mean velocity through the tube and S_W, swirl number (Yokoya et al., 1994).

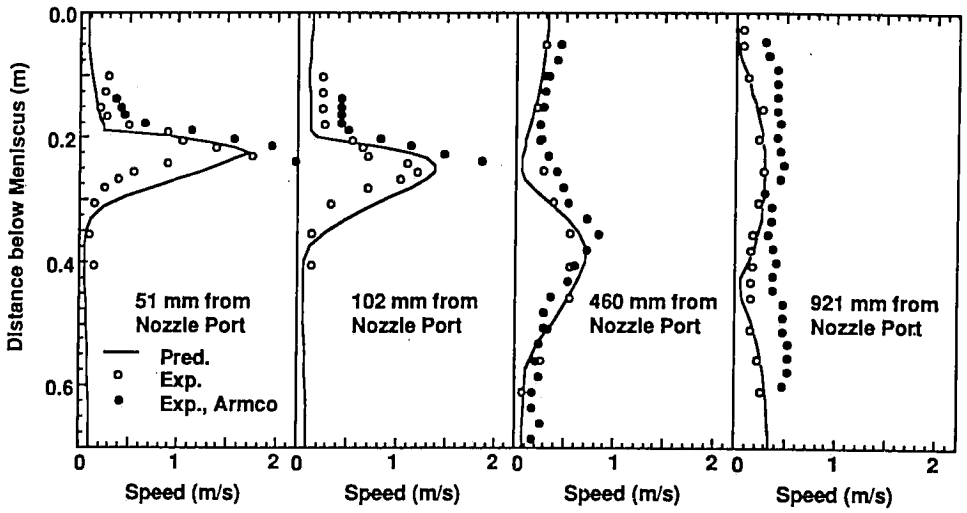

Fig. 11: Predicted and measured water speeds in a physical model of a continnuous caster. Results of Thomas and colleagues (1994).

An exemplary study of flow in tundishes is that of Shen et al. (1994). This was both mathematical and physical (water) modeling of a tundish for use in aluminum casting. LDV and laser sheet visualization were used on the experimental apparatus. The CFD relied on the k-ε model in what was a formidable geometry with inclined walls, turns and irregular cross sections. Figure 12 indicates the success of the CFD; these results are for a vertical section were the metal flows in through a nozzle on the upper left. These workers were also able to accurately calculate turbulence quantities such as the sum of the time averaged values of the squares of two fluctuating velocity components (see Figure 13).

The CFD of tundishes has long been an interest of Sahai's group. One of the recent contributions is the paper by Damle and Sahai (1995) who carried out both calculations and measurements (on a water model) of the effect of tracer density on the flow. Tracers have been used frequently in water models and actual tundishes to characterize the flow (residence time distributions, etc.). These investigators examined the question of whether tracers of somewhat different density than the liquid under study could lead to erroneous results i.e. to a flow field different from that of this liquid. Calculations were carried out using the k-ε model and a mass transport equation wherein the effective diffusivity was obtained from an assumption of one for the effective Schmidt number. Figure 14 shows computed velocities for the 50 minutes after addition of a pulse of tracer to the water model. Clearly the computed results show that this tracer seriously distorts the flow in the tundish. [The mean residence time of the water was 999 seconds so that the flow at 3000 sec. was close to the true one.]

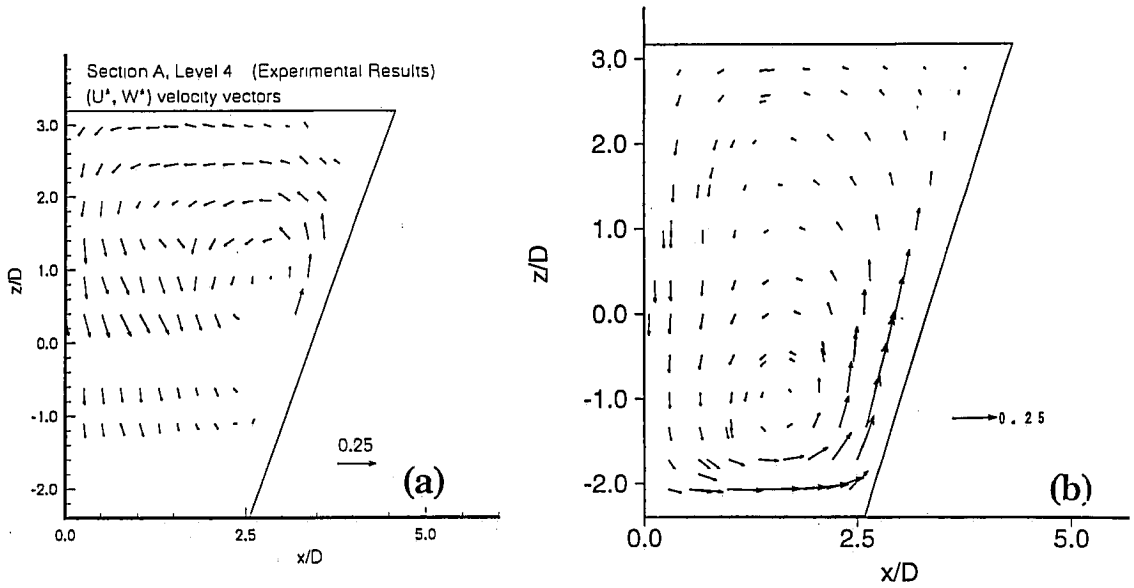

Fig. 12: Measured (a) and predicted (b) velocities for vertical planes in a tundish from the paper of Shen et al. (1994).

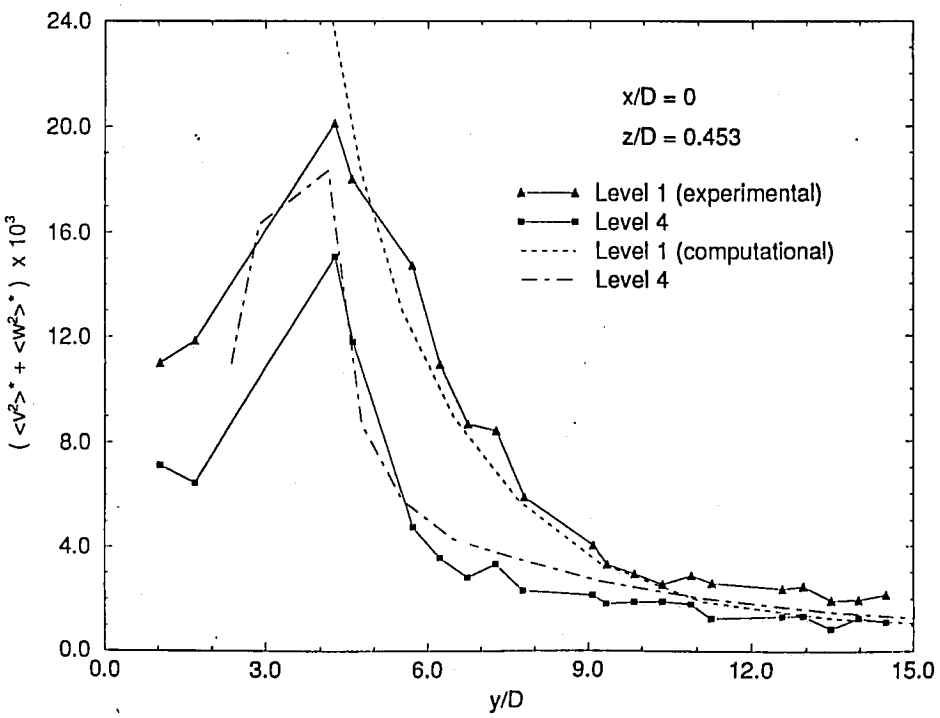

Fig. 13: Variation of ($\langle v^2 \rangle^* + \langle w^2 \rangle^*$) in the flow direction on plane M for both tundishes near the bottom wall. (Shen et al., 1994).

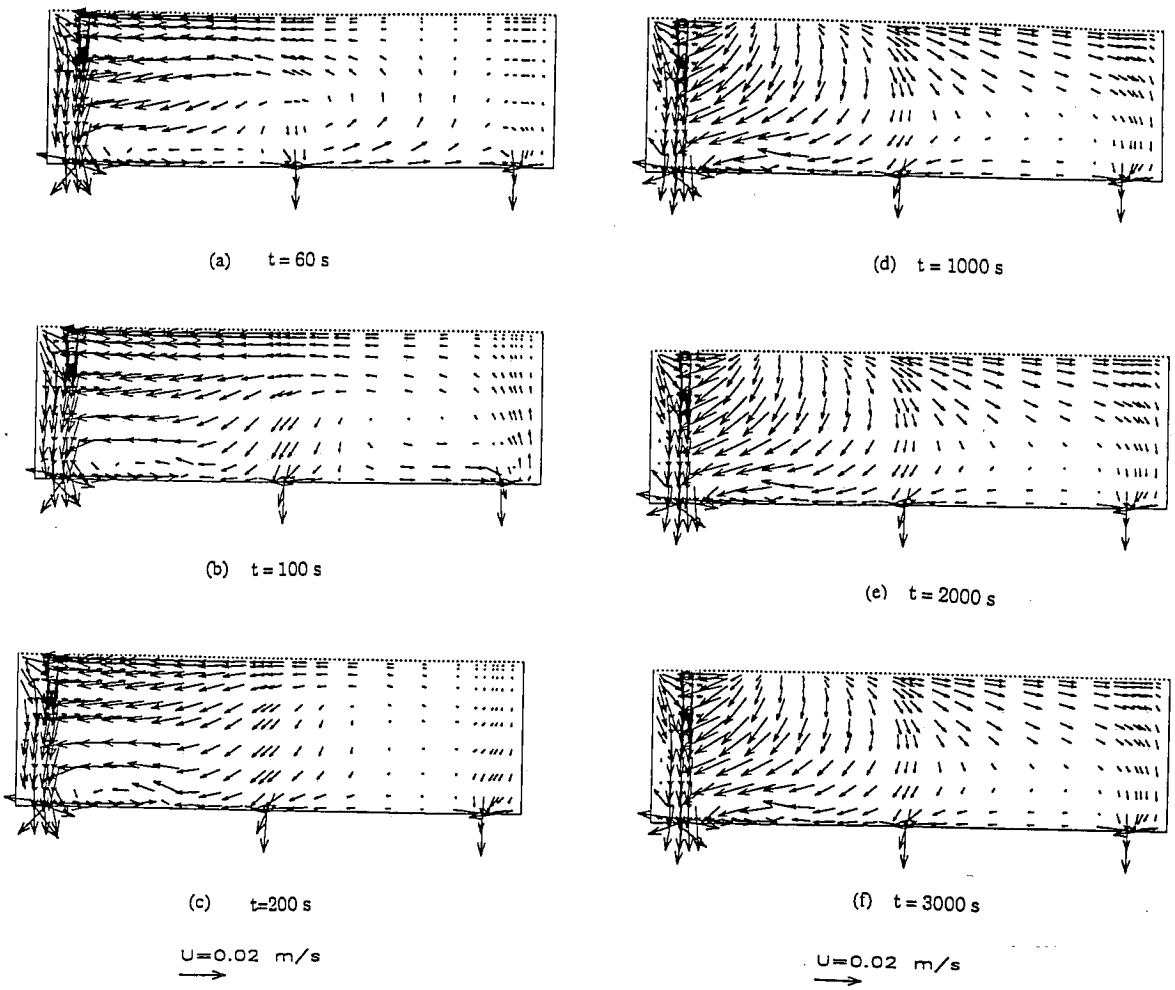

Fig. 14: Velocity profiles in the symmetry plane of the tundish at different time intervals from the injection of the saturated KCl solution tracer. (Damle and Sahai, 1995)

Other recent papers on the CFD of tundishes are those of Barreto-Sandeval et al. (1996a,b), of Chen and Pehlke (1996), and of Ilegbusi (1994) the last incorporating an unusual turbulence model, rather than the k-ε model that has held sway in the papers discussed so far. O'Connor and Dantzig (1994) have done calculations on a thin slab caster and went on to model heat transport and the stresses developed in the irregularly shaped mold.

One may conclude from the publications described above (and others too numerous to mention), that for the prediction of time averaged velocities, and perhaps of turbulence quantities, in many unit operations of the metallurgical industries, CFD has provided us with robust tools. There are exceptions, for example recent work by Baake et al. (1995) suggest that significant modification of the k-ε model is required if it is to predict the turbulent viscosity in inductively stirred melts, although the time averaged velocities of their experiments were well predicted, in line with earlier calculations by Lympany and Evans (1983).

A recent interesting paper where there is departure from the usual norm of k-ε modeling is that of Lan and coworkers (1997). These investigators carried out extensive measurements of time-averaged velocity and turbulence kinetic energy in a cylindrical water model of a continuous caster using LDV. The results were then compared to the predictions of the usual (high Reynolds number) k-ε model and to those of five low Re versions. Representative results appear in Figure 15 where it is seen that the mean (time-averaged) velocity along the axis is well predicted by all models, except one of the low Re models. The usual high Re model (HR in Figure 15) giving good results, it is the clear choice among these models, based on the mean velocity, because the number of iterations and the CPU time per iteration are both far lower than for other models. However all the models are somewhat deficient in predicting the turbulence kinetic energy and the authors ascribe this shortcoming to the anisotropy of the turbulence revealed by their measurements.

In the next section the author makes suggestions of non-routine problems where there are opportunities for advancement in the next few years.

3. OPPORTUNITIES FOR ADVANCEMENT WITH CFD

3.1 Free surface behavior

Free surfaces and liquid-liquid interfaces occur in metal processing operations and their behavior has been relatively neglected by the computational fluid dynamicist. Technologically important examples include the deformation of the aluminum-electrolyte interface in Hall-Heroult cells used to produce aluminum (e.g., Wahnsiedler, 1987), the impact of droplets with solid surfaces such as occurs in spray forming (e.g., Ilegbusi and Szekely, 1994; Hatta et al., 1995, Rein, 1993, Fukai et al., 1993), and the perturbation of otherwise smooth surfaces by mechanical devices (Sha et al., 1996)) or electromagnetic forces (Ilegbusi and Szekely, 1994; Deepak and Evans, 1995; Kageyama and Evans, 1997) in casting processes. In many instances the dynamics of the surface are dependent on a flow adjacent to the surface that is turbulent and the application of conventional turbulence modeling under those circumstances is questionable. Given this difficulty and the fact that the surface behavior is frequently three-dimensional, this neglect is understandable.

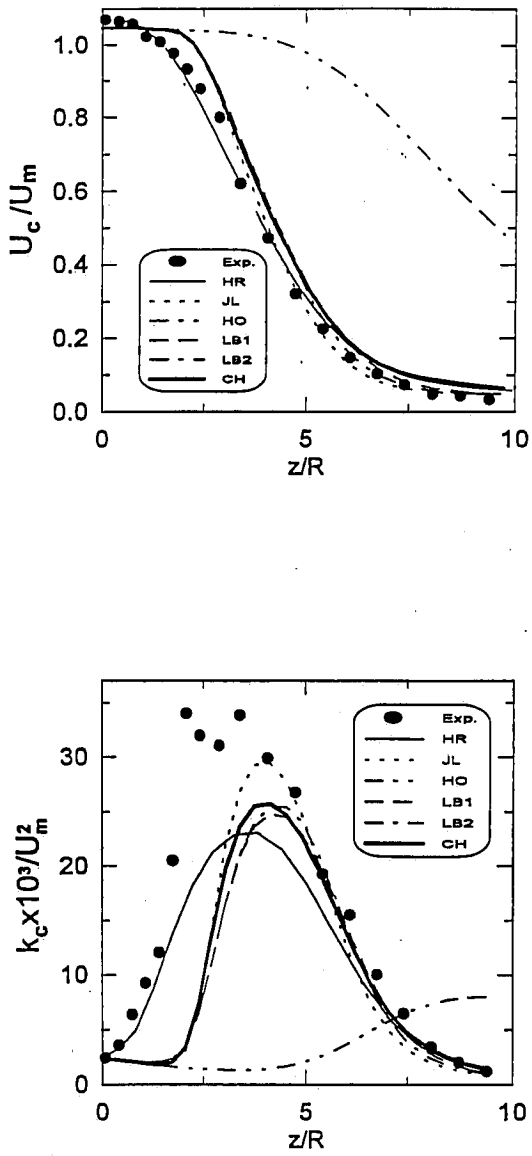

Fig. 15: Comparison of the measured to predicted (upper) axial mean velocity and (lower) turbulence kinetic energy, along the symmetry axis (Lan et al., 1997).

A recent study on the dynamic behavior of the interface between two liquids is that of Sha and coworkers (1996). This investigation appears to have been oriented towards continuous casting of steel where the mold is oscillated vertically at a frequency of a few Hz; a cylindrical mercury pool surmounted by a similar pool of silicone oil was confined within a plastic mold oscillating vertically at a frequency of 2 Hz. These investigators solved the (instantaneous)

continuity and Navier-Stokes equations for this system with careful treatment of the triple phase (oil-mercury-plastic) line (TPL). The marker and cell (MAC) approach was used to follow the movement of the interface and oil free surface. Fig 16 shows the comparison between the authors' measurements of the position of the TPL and their computations.

Kageyama and Evans (1997), following the linear perturbation analysis of Deepak and Evans (1995), have examined the dynamic behavior of the surface of a metal pool subjected to electromagnetic forces. Electromagnetic casting was the application that these investigators saw for their results (described in more detail elsewhere in these proceedings). The instantaneous continuity/N-S equations were solved for the pool with recomputation of the electromagnetic force as the shape of the free surface changed.

Both experimental and computational work was carried out by Hatta et al. (1995) on the impact of (water) droplets with a solid surface. Second order finite difference methods were coupled with MAC calculations to yield the good agreement between measured and computed drop dimensions seen in Figure 17. Calculations of this kind had been carried out earlier by Trapaga et al. (1992).

3.2 Fluid flow and microstructure development

An even greater opportunity may be exploration of the link between flow during solidification and the microstructure/ microchemistry of the resulting material. Until recently there has been a gulf between CFD and materials science. The achievements of CFD in process metallurgy described above have taught us much about engineering (maximizing productivity, conserving energy, design of equipment, etc.) but nothing about the structure/properties which are the paradigm of the materials scientist and the users of the products of the process metallurgist. For many years there have been numerical studies of flow and transport at the macroscopic level during solidification; examples are from the groups of Voller (1989), Dantzig (1989), Thomas (Najjar et al., 1995), Cross (Chow et al., 1995), Poirier (1991) and Beckermann (Wang and Beckermann, 1995).

There are also many treatments of transport and other fundamental phenomena occurring at the microscopic level during solidification in the absence of flow (Kurz and Fisher, 1992; Rappaz, 1989; Stefanescu, 1995; Gandin et al., 1995). However, computational research into flow and solidification at the scale of the microstructure has been rare. For example, a recent special issue (no. 6, 1995) of ISIJ International, devoted to recent advances in solidification, contains 37 papers, but only one of these embraces CFD.

Dantzig et al. (1987) have carried out calculations for one cell in a solidifying cellular structure subject to shear flow. Three-dimensional velocity, temperature and concentration fields were calculated, using finite elements, in the melt flowing past the solid; the cellular interface was found to translate into the flow approach direction, consistent with the experimental observations of others.

Another example of the treatment of flow at the microscopic level is the work of Bhat and coworkers (1995). Lead-tin alloys were quenched after partial solidification and the dendritic structures characterized by means of image analysis of micrographs. The digitized images were then used to prepare a finite element mesh which was subsequently used in CFD (in two dimensions) to determine the permeability of the mushy zone the instant before quenching. Figure 18 is an example of the computed flow field in this highly irregular geometry.

While this was an impressive computational undertaking the extension of the work to 3-D flows seems worthwhile. Such an extension is rendered difficult by the highly irregular structure of the dendritic region in three dimensions. McCarthy (1994) has described an approach that might be more readily extended to 3-D interdendritic flow: computations of flow using cellular automata. While McCarthy's published results pertain to 2-D flows through regular and random arrays of simple shapes (cylinders and cruciforms), the power of the technique and prospects for its extension to 3-D interdendritic flows are apparent. The fluid dynamicist can be relieved that these flows are not turbulent; Taniguchi and Evans (1993) have shown experimentally that turbulence can only penetrate cavities if the length scale is smaller than the cavity width (an unlikely case for most dendrite arm spacings).

Very recently Beckerman (1997) has published an overview of the modeling of segregation and grain structure development in solidification with convection.

4. CONCLUDING REMARKS

In this paper the author has attempted to show that, for many metals processing operations, CFD has now provided a means for incorporating the important effects of fluid flow into quantitative descriptions of process behavior. While, no doubt, there are incremental improvements to be made, in turbulence modeling for example, the major unit operations have been treated by CFD. Two relatively unexplored areas of process behavior appear to be operations where free surfaces or interfaces are significant and the many phenomena, affected by flow, that determine the microstructure and properties of cast metals. These unexplored areas, and others will provide opportunities in CFD to make a valuable contribution to the technology of metals processing in the next decade.

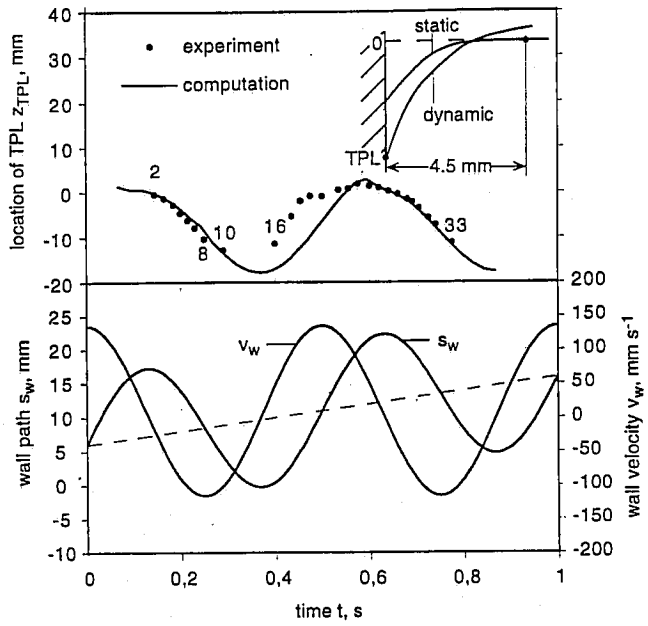

Fig. 16: Movement of the triple phase line wall/oil/mercury. The reference point is the z coordinate of the static meniscus at a distance x = 4.5 mm from the wall. Work of Sha et al., 1996.

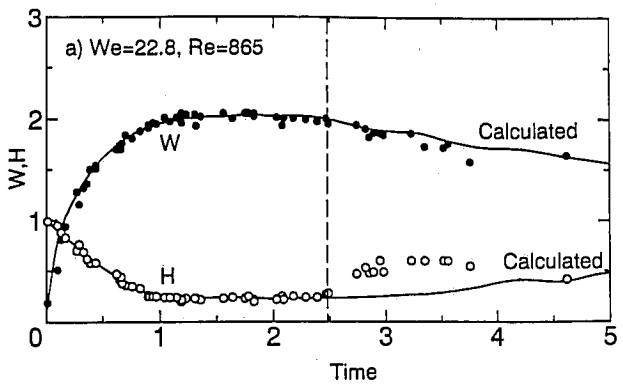

Fig. 17: Computed and measured droplet widths and heights during impact with a solid surface. Work of Hatta et al. (1995).

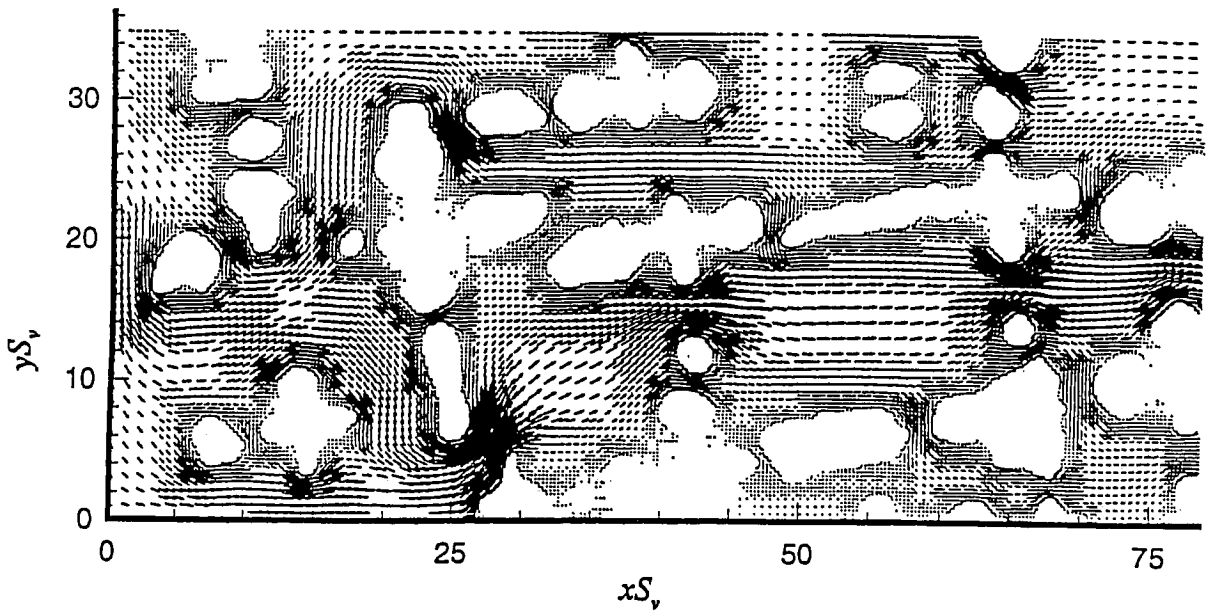

Fig. 18: Velocity vector plot for flow through a digitized image of a microstructure. Calculations of Bhat et al. (1995).

REFERENCES

Baake, E., A. Mühlbauer, A. Jakowitsch and W. Andree, 1995, Metall. Trans., 26B, pp. 529-536.

Barreto, J. de J., M. A. Barrón Meza and R. D. Morales, 1996, ISIJ International, 36, pp. 543-552.

Barreto, J. de J., A. W. D. Hills, M. A. Barrón Meza and R. D. Morales, 1996, ISIJ International, 36, pp. 1174-1183.

Beckerman, C., 1997, J. Metals, 49, pp. 13-17.

Bhat, M. S., D. R. Poirier and J. C. Heinrich, 1995, Metall. Trans. , 26B, pp. 1049-1056.

Castillejos, A. H. and J. K. Brimacombe, 1987, Metall. Trans., 18B, pp. 649-658 and pp. 659-671.

Castillejos, A. H. and J. K. Brimacombe, 1989, Metall. Trans., 20B, pp. 595-601.

Chen, H. S. and R. D. Pehlke, 1996, Metall. Trans., 27B, pp. 745-756.

Chow, P., C. Bailey, M. Cross and K. Pericleous, p. 213 in Modeling of Casting, Welding and Advanced Solidification Processes, M. Cross and J. Campbell, eds., TMS, Warrendale PA 1995.

Damle, C. and Y. Sahai, 1995, ISIJ International, pp. 163-169.

Dantzig, J. A., L. S. Chao and I. Lekadis, 1987, Proc. 1987 ASME-JSME Thermal Engineering Joint Conference, ASME, 3, p. 251.

Dantzig, J. A., 1989, Int. J. Numerical Meth. in Eng., 28 pp. 1769.

Deepak, G. and J. W. Evans, J. Fluid Mech., 1995, 287, pp. 133-150.

J. Fukai, Z. Zhao, D. Poulikakos, C. M. Megaridis and O. Miyatake, 1993, Phys. Fluids A, 5, pp. 2588-2599.

Gandin, Ch.-A., Ch. Charbon and M. Rappaz, 1995, ISIJ Int., 35, pp. 651-657.

Hatta, N. et al., 1995, ISIJ Int., 35, pp. 1094-1099.

Ho, Y.-H., C.-H. Chen and W.-S. Hwang, 1994, ISIJ International, 34, pp. 255-264.

Iguchi, M., H. Kawabata, K. Nakajima and Z.-I. Morita, 1995, Met. and Mat. Trans., 26, pp. 67-74.

Iguchi, M., et al., 1995, Metall. Trans., 26B, pp. 241-247.

Iguchi, M., H. Ueda, T. Chihara and Z. Morita, 1996, Metall. Trans., 27B, pp. 765-772.

Iguchi, M., T. Nakatani and H. Ueda, 1997, Metall. Trans., 28B, pp. 87-94.

Ilegbusi, O. J., 1994, ISIJ International, 34, pp. 734-738.

Ilegbusi, O. J. and J. Szekely, 1994, ISIJ Int., 34, pp. 943-950.

Jonsson, L. and P. Jönsson, 1996, ISIJ International, 9, pp. 1127-1134.

Kageyama, R. and J. W. Evans, "Computation of the oscillation of free surfaces and the effect of electromagnetic fields", these proceedings.
Kurz, W. and D. J. Fisher, 1992, Fundamentals of Solidification, Trans Tech Publications, Switzerland.
Lan, X. K., J. M. Khodadadi and F. Shen, 1997, Metall. and Mat. Trans., 28B, to appear.
Lympany, S. D. and J. W. Evans, 1983, Metall. Trans., 14B, pp. 306-308.
Mazumdar, D. and R. I. L. Guthrie, 1995, ISIJ International, 35, pp. 1-20.
Mazumdar, D. and R. I. L. Guthrie, 1994, Metall. Trans., 25B, pp. 308-312.
Mazumdar, D., R. I. L. Guthrie and Y. Sahai, 1993, Appl. Math. Model., 17, p. 255
McCarthy, J. C., 1994, Acta Metall. Mater., 31 , p. 1573.
McDavid, R. M. and B. G. Thomas, 1996, Metall. Trans., 27B, pp. 672-685.
Mietz, J. and F. Oeters, 1989, Steel Res., 60, p. 387.
Najjar, F., B. G. Thomas and D. E. Hershey, 1995, Metall. Trans., 26B, pp. 749-765.
Najjar, F. M., B. G. Thomas and D. E. Hershey, 1995, Metall. and Mater. Trans. 26B , p. 749.
Poirier, D. R., P. J. Nandapurkar and S. Ganesan, 1991, Metall. and Mater. Trans., 22B, p. 889.
Prasso, D., J. W. Evans and I. J. Wilson, 1996, Metall. Trans., 26B, pp. 1243-1251.
Rappaz, M., 1989, Int. Mater. Rev., 34, p. 93.
Rein, M., 1993, Fluid Dynamics Research, 12, pp. 61-93.
Sahai, Y. and R. I. L. Guthrie, 1982, Metall. Trans., 13B, pp. 203-
Sha, H., R. Diedrichs and K. Schwerdtfeger, 1996, Metall. Trans., 27B, pp. 305-314.
Shen, F., J. M. Khodadadi, S. J. Pien, and X. K. Lan, 1994, Metall. Trans., 25B, pp. 669-680.
Sheng, Y. Y. and G. A. Irons, 1995, Metall. Trans., 26B, pp. 625-635.
Sheng, Y. Y. and G. A. Irons, 1992, Metall. Trans., 23B, p. 779
Singh, A. K. and D. Mazumdar, 1997, Metall. Trans., 28B, pp. 95-102.
Stefanescu, D. M., 1995, ISIJ Int., 35, pp. 637-650.
Szekely, J. H. J. Wang and K. M. Kiser, 1976, Metall. Trans., 7B, p. 287
Szekely, J. and R. T. Yadoya, 1972, Metall. Trans., 3, p. 2673
Szekely, J. and R. T. Yadoya, 1973, Metall. Trans., 4, p. 1379
Taniguchi, Y. and J. W. Evans, 1993, Int. J. Heat Mass Trans., 36, pp. 951-965.
Tarapore, E. D. and J. W. Evans, 1976, Metall. Trans., 7B, pp. 343-351.
Thomas, B. G., X. Huang and R. C. Sussman, 1994, Metall. Trans., 25B, pp. 527-547.
Trapaga, G., E. F. Mathys, J. J. Valencia and J. Szekely, 1992, Metall. Trans., 23B, p. 42.
Voller, V. R. and A. D. Brent, 1989, Int. J. Heat Mass Transfer, 32, pp. 1719.
Wahnsiedler, W. E., 1987, TMS, Warrendale PA, pp. 269-287.
Wang, C. Y., and C. Beckermann, 1995, p. 549 in Modeling of Casting, Welding and Advanced Solidification Processes, M. Cross and J. Campbell, eds., TMS, Warrendale PA
Yokoya, Y. Asako, S. Hara and J. Szekely, 1994, ISIJ International, 34, pp. 883-888.
Yokoya, Y. et al., ISIJ International, 34, pp. 889-895.
Zhu, M.-Y., T. Inomoto, I. Sawada and T-C. Hsiao, 1995, ISIJ International, 35, pp. 472-479.
Zhu, M.-Y., I. Sawada, N. Yamasaki and T-C. Hsiao, 1996, ISIJ International, 5, pp. 503-511.
Ziegler, D. and J. W. Evans, 1986, J. Electrochem. Soc., 133, pp. 567-575.